

Intracrystalline Transformation of Olivine to Wadsleyite and Ringwoodite Under Subduction Zone Conditions

Ljuba Kerschhofer, Thomas G. Sharp, David C. Rubie

Experiments on $\text{Mg}_{1.8}\text{Fe}_{0.2}\text{SiO}_4$ olivine at 18 to 20 gigapascals and 1000° to 1400°C show that transformation to the high-pressure polymorphs wadsleyite and ringwoodite involves two competing nucleation mechanisms when the grain size of the olivine is large: (i) incoherent nucleation on olivine grain boundaries and (ii) coherent intracrystalline nucleation of ringwoodite lamellae on shear-induced stacking faults in olivine on the (100) planes, followed by the nucleation of wadsleyite on the ringwoodite. The large amount of intracrystalline transformation, which occurs under low differential stress under the pressure and temperature conditions of the mantle transition zone, suggests that shear-induced intracrystalline transformation of olivine to wadsleyite and ringwoodite is important in subducting slabs.

The polymorphic phase transformation of olivine (α phase) to its high-pressure polymorphs wadsleyite (β phase) and ringwoodite (γ phase) is likely to be kinetically inhibited in subduction zones because of low temperatures (1, 2). As a consequence, olivine would persist metastably within a wedge-shaped region to depths below 400 km, where the equilibrium breakdown of olivine is expected to occur. A wedge of metastable olivine in subducting slabs may be important for the dynamics of subduction in view of its potential effects on the buoyancy forces and on the rheology and state of stress within the slab (2–4). Furthermore, the development of a shear instability through the rapid transformation of metastable olivine has been proposed as the cause of deep-focus earthquakes (2, 4–7).

To test the metastable olivine hypothesis, we must understand the mechanisms and kinetics of the α - β - γ transformations. Investigations on natural ringwoodite and wadsleyite in meteorites (8, 9) as well as experimental studies at high pressure have been carried out to elucidate the nature of these transitions. Most experiments have been performed on analog compositions such as Mg_2GeO_4 , Ni_2SiO_4 , Fe_2SiO_4 , Mg_2SiO_4 , and Co_2SiO_4 (10–16). These studies indicate that the α -to- γ transformation can occur either by incoherent grain boundary nucleation and interface-controlled growth (17), when differential stresses are low and the pressure is fairly close to equilibrium (10, 11, 13, 16), or by an intracrystalline mechanism that is presumed to involve shear (10–12, 14, 15, 18). It was predicted theoretically (19) that the latter mechanism involves the migration of partial dislocations of the

type $1/12[013]$ and $1/12[0\bar{1}3]$, which creates stacking faults in the (100) plane of olivine. The shear is accompanied by the coordinated movement of the cations in the faulted structure, which results in a layer of γ -phase structure in the olivine (19). Theoretically, the transformations from α to γ and α to β by means of a hypothetical intermediate phase ϵ^* are possible by such a “martensitic-like” or shear mechanism (8). In contrast to grain boundary nucleation, the shear mechanism has only been observed to occur experimentally when the differential stress is high ($\sigma_1 - \sigma_3 \geq 1$ GPa) or when the pressure overstep of equilibrium conditions is large (for example, $\Delta P \geq 8$ GPa) (10–12, 18). Because differential stresses and pressure oversteps of the above magnitudes are probably unrealistic for subduction zones, kinetic models of the α - β - γ transformations in subducting slabs have been based mainly on the incoherent grain boundary nucleation mechanism (1, 2). We show here that the transformation can be initiated by a shear mechanism with subsequent intracrystalline nucleation and growth of the γ phase or β phase occurring on stacking faults in olivine under conditions of pressure, temperature, and stress appropriate for subduction zones.

We performed experiments on $\text{Mg}_{1.8}\text{Fe}_{0.2}\text{SiO}_4$ San Carlos olivine using a 1200-metric ton multianvil press (20). The samples consisted of an oriented single crystal (500 μm by 600 μm by 700 μm) that was embedded in a fine-grained (10 to 20 μm) matrix of San Carlos olivine powder plus 4 weight % San Carlos enstatite (21). The pressure-temperature-time (P - T - t) paths of all experiments in relation to the α - β - γ equilibrium phase boundaries (22) are shown in Fig. 1. We commenced each experiment by hot-pressing the sample in the

olivine stability field (1200°C, 11 GPa, 3 hours) to produce an equilibrated microstructure with low dislocation densities in the initially powdered material (23). After hot-pressing, we changed the P - T conditions to initiate transformation to the high-pressure phases. During this transformation stage, the samples were reacted at various P - T conditions, nominally in the γ -stability field (Fig. 1). After quenching and decompression, the samples were prepared for examination by optical and transmission electron microscopy (TEM).

Optical and TEM observations show that the β phase or γ phase nucleated incoherently on olivine grain boundaries in all samples reacted at $\geq 1000^\circ\text{C}$ (Table 1) (24, 25). All reacted single crystals (except Ol 31) are surrounded by sharply defined reaction rims, up to 22 μm wide, consisting largely of β -phase grains in random orientations that nucleated incoherently (Fig. 2, A and B). The widths of the reaction rims, measured as a function of time, show that the growth rate at 1100°C and 18 GPa decreases with time and that growth may eventually stop (samples Ol 32, Ol 22, Ol 24). The reason for the decreasing growth rates is not yet clear but has potentially important implications for competing transformation mechanisms. The fine-grained olivine matrix also transformed by incoherent grain boundary nucleation and growth, thus resulting in a fine-grained mixture of

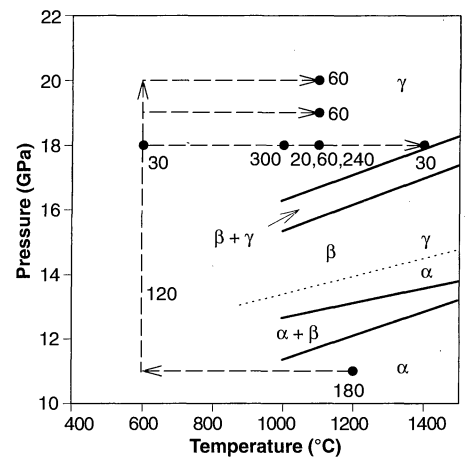


Fig. 1. Phase diagram for $\text{Mg}_{1.8}\text{Fe}_{0.2}\text{SiO}_4$ showing the stability fields of olivine (α), the β phase (β), and the γ phase (γ) [after (22)]. In addition to the equilibrium boundaries (solid lines), the calculated metastable α - γ boundary (28) is shown (dotted line). The dashed arrows indicate the P - T - t paths for our experiments. Numbers refer to the durations of each stage (in minutes). After hot pressing, we reduced the temperature to 600°C to avoid transforming the sample during the subsequent pressurization to 18 to 20 GPa. Heating to the final temperature was relatively rapid (about 2 min), thus making it possible to define the P - T - t conditions at which the transformation began.

the β and γ phases.

Optically visible, lens-shaped inclusions consisting predominantly of the β phase are present at intracrystalline sites in the reacted olivine single crystals. The planes of the lenses are parallel to the (101) planes of the olivine crystal (Fig. 2). In addition to these large lenses, TEM observations showed that thin plate-like lamellae of the γ phase, oriented parallel to $(100)_\alpha$, are present within the olivine crystals (Fig. 3A). These lamellae range from ten to several tens of nanometers wide and from tens of nanometers up to several micrometers long. The γ -phase lamellae have a crystallographic orientation relation to olivine in which the close-packed planes $(100)_\alpha$ and $\{111\}_\gamma$ are parallel and the directions $[001]_\alpha$ and $\langle 110 \rangle_\gamma$ are collinear (Fig. 3A).

We investigated the morphology of the γ -phase lamellae and the α - γ interface at the nanometer scale using high-resolution (HR) TEM. We observed planar defects in the $(100)_\alpha$ plane that commonly occur in pairs, separated by only one or two unit cells of olivine (Fig. 3B). Diffraction contrast imaging reveals that these planar de-

fects are terminated by partial dislocations and are therefore stacking faults in the $(100)_\alpha$ plane. Many γ -phase lamellae are associated with such stacking faults, with the faults extending beyond the ends of the lamellae, whereas other lamellae are apparently not associated with stacking faults (Fig. 3B).

Lamellae of the γ phase in olivine with the orientation relation $(100)_\alpha // \{111\}_\gamma$ have been observed (10–12, 14, 15, 18). On the basis of this crystallographic relation, these

authors concluded that the lamellae formed by the shear mechanism predicted in (19). Our observations of γ -phase lamellae growing on stacking faults in olivine provide additional evidence for such a mechanism. However, a sample that has partially transformed exclusively by a shear mechanism should consist of unit-cell-scale lamellae that grow in number as the transformation progresses. In contrast, most γ -phase lamellae in our samples are tens of nanometers wide, have rounded ends, and appear to be

Table 1. Pressure-temperature-time conditions of multianvil experiments and results (from optical microscopy). RR, reaction rim (with width); IN, intracrystalline nucleation.

Run number	P (GPa)	T (°C)	t (min)	Results
OI 31	18	600	30	α , low dislocation density
OI 25	18	1000	300	α + RR (22 μm) + IN
OI 32	18	1100	20	α + RR (12 μm) + IN
OI 22	18	1100	60	α + RR (22 μm) + IN
OI 24	18	1100	240	α + RR (22 μm) + IN
OI 30	18	1400	30	β^*
OI 26	19	1100	60	α + RR (20 μm) + IN
OI 27	20	1100	60	α + RR (12 μm) + IN

*100% transformation with textures suggesting IN.

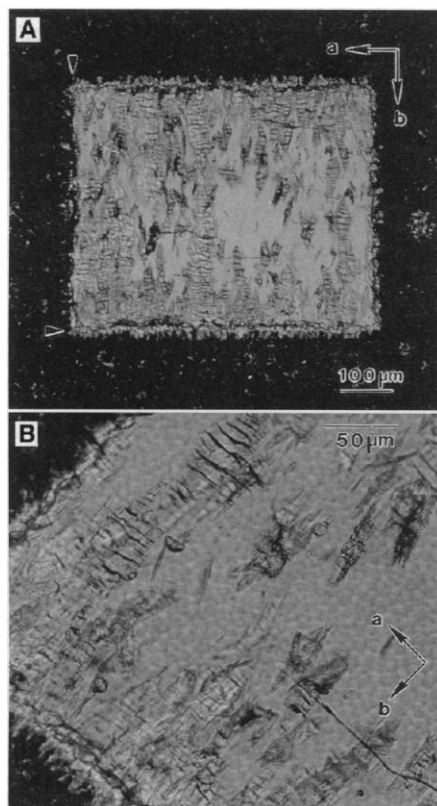


Fig. 2. (A) Optical micrograph (crossed Nicol prisms) of a reacted olivine single crystal (OI 26) viewed along the c direction, showing a reaction rim (20 μm wide) around the crystal (arrowheads). Many lenses consisting predominantly of the β phase are visible within the crystal. (B) Magnified view of a detail of (A) showing the intracrystalline lenses.

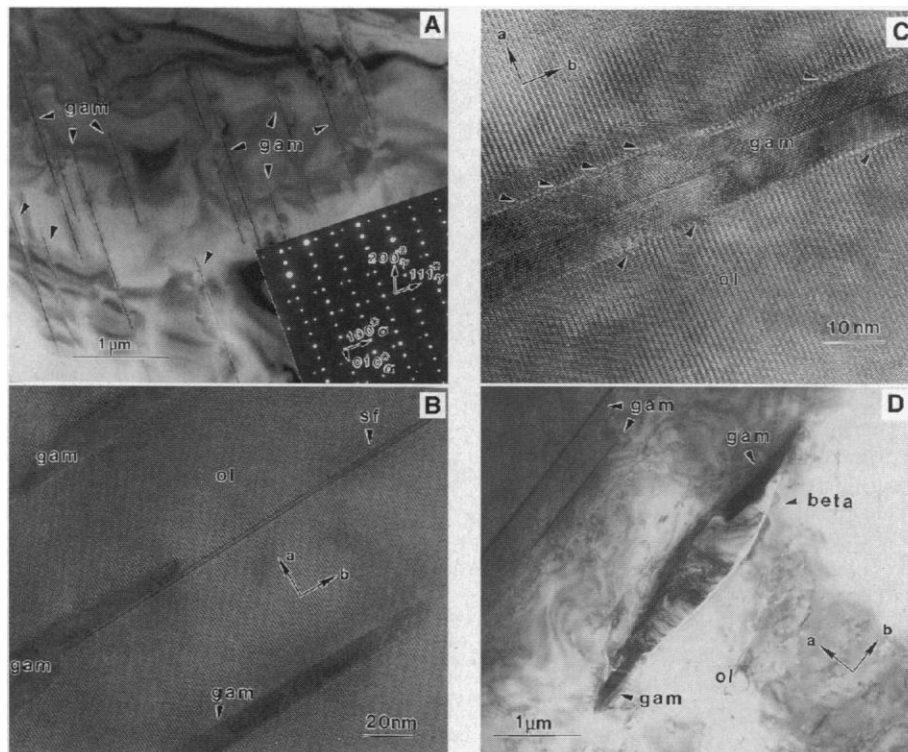


Fig. 3. (A) Bright-field TEM image of olivine containing γ -phase lamellae (gam) oriented parallel to the (100) plane of olivine. (Inset) Electron diffraction pattern of the olivine $[001]_\alpha$ and γ -phase $\{110\}_\gamma$ zone axes showing the crystallographic orientation relation $[100]_\alpha^* // \langle 111 \rangle_\gamma^*$. (B) HRTEM image of a pair of stacking faults (sf) extending out of a twinned γ -phase lamella with the two halves of a twinned lamella growing along the two faults. The arrows indicate the crystallographic orientation of the olivine (ol). (C) HRTEM image of a twinned γ -phase lamella as indicated by the symmetric arrangement of $\{110\}$ stacking faults (arrowheads) on either side of the lamella. (D) Bright-field image of an incoherent β -phase lens (beta) oriented along the b direction of olivine. The two dark areas at the tips of this lens consist of the γ phase, showing the same orientation relation with olivine as in (A). Two narrow γ -phase lamellae are also visible.

structurally distinct from the stacking faults (Fig. 3B). In addition, we observed steps that are one or two olivine unit cells in height along α - γ interfaces (Fig. 3C). Many of the γ -phase lamellae are twinned with a coherent twinning plane $\{111\}_\gamma$ that is parallel to $(100)_\alpha$ (Fig. 3C).

These observations indicate that the transformation occurs in two stages. The first stage involves a shear mechanism, similar to that proposed in (19), which produces stacking faults in the olivine. The second stage involves the coherent nucleation and growth of the γ phase on these stacking faults. Indications of the growth process include the rounded ends of the lamellae (as opposed to layers of faulted material), steps on the α - γ interfaces, and the numerous stacking faults in the $\{110\}_\gamma$ planes, which are probably growth features (Fig. 3C). Two γ grains that nucleate and grow on both sides of a fault or on a pair of closely spaced stacking faults, which may have opposite shear directions (Fig. 3B), result in a twinned lamella (Fig. 3C). Analytical TEM shows that the chemical compositions of the α phase and γ phase are the same within analytical error, which suggests that the growth of the γ -phase lamellae is interface-controlled.

TEM observations show that the β phase occurs in contact with the γ phase (Fig. 3D), suggesting that the β -phase grains nucleate on previously formed γ -phase grains and are precursors to the larger, optically visible lenses (Fig. 2A). We observed no crystallographic relation between the β and α phases in our samples. This is not surprising because numerical calculations indicate that coherent intracrystalline nucleation of the β phase in olivine is unlikely because of the large elastic strain energy involved (26). The intracrystalline formation of incoherent lenses of wadsleyite in our olivine single crystals is similar to the coarsening of γ - Mg_2GeO_4 lamellae (5), although the β structure does not exist in the Mg_2GeO_4 system.

We have used the dislocation density of an olivine single crystal (Ol 31), which was annealed at 18 GPa and 600°C without transforming, to estimate the differential stress under our experimental conditions. On the basis of the dislocation density versus stress calibration of (27), the observed dislocation density of 10^7 cm^{-2} indicates that the differential stress in our samples was ~ 30 MPa. This result demonstrates that high differential stresses are not necessary for a shear mechanism to be activated in natural olivine, as was also concluded for Mg_2GeO_4 (12). On the other hand, a large pressure overstep may be necessary, as suggested by the Mg_2GeO_4 study in which

α -to- γ shear transformation occurred at a pressure overstep of 8 to 14 GPa (12). Our experimental conditions overstep the metastable α - γ phase boundary by 4 to 6 GPa (Fig. 1), which is realistic for subduction zones.

Our results indicate that intracrystalline and grain boundary transformation mechanisms are competing processes and that intracrystalline transformation dominates in the large crystals after a certain reaction time. Investigations of the fine-grained olivine after partial transformation showed no evidence of intracrystalline nucleation, probably because incoherent nucleation and growth on grain boundaries is fast enough to consume the small grains before intracrystalline transformation dominates. Even if intracrystalline nucleation rates are much slower than grain boundary nucleation rates, the overall transformation by an intracrystalline mechanism can dominate if growth rates are slow (26). This is so because intracrystalline nuclei can be closely spaced within olivine grains. In contrast, in the grain boundary nucleation mechanism, nuclei are located on relatively widely spaced grain boundaries. In the intracrystalline nucleation case, the growth distances required for complete transformation are much smaller than in the grain boundary nucleation case, and the transformation kinetics will therefore be very different (26). Intracrystalline transformation will be particularly important when the grain size of the olivine starting material is large, as is likely to be the case in subducting lithosphere. Current thermokinetic models of the α - β - γ transformations (1, 2), which are based only on the incoherent grain boundary nucleation mechanism, may therefore be inadequate for predicting the depth of olivine metastability in subduction zones.

REFERENCES AND NOTES

- C. M. Sung and R. G. Burns, *Tectonophysics* **31**, 1 (1976); D. C. Rubie and C. R. Ross, *Phys. Earth Planet. Inter.* **86**, 223 (1994); R. Daessler, D. A. Yuen, S. Karato, M. R. Riedel, *ibid.* **94**, 217 (1996).
- S. H. Kirby, S. Stein, E. A. Okal, D. C. Rubie, *Rev. Geophys.* **34**, 261 (1996).
- M. R. Riedel and S. Karato, *Geophys. J. Int.* **125**, 397 (1996).
- S. H. Kirby, W. B. Durham, L. A. Stern, *Science* **252**, 216 (1991).
- H. W. Green II and P. C. Burnley, *Nature* **341**, 733 (1989).
- P. C. Burnley, H. W. Green II, D. Prior, *J. Geophys. Res.* **96**, 425 (1991).
- S. H. Kirby, *ibid.* **92**, 13789 (1987).
- M. Madon and J. P. Poirier, *Phys. Earth Planet. Inter.* **33**, 31 (1983).
- G. D. Price, A. Putnis, D. G. W. Smith, *Nature* **296**, 729 (1982).
- P. C. Burnley, thesis, University of California, Davis (1990).
- _____ and H. W. Green II, *Nature* **338**, 753 (1989).
- P. C. Burnley, *Am. Mineral.* **80**, 1293 (1995). In that study, large amounts of transformation, inferred to occur by the shear mechanism of (19), resulted at pressure oversteps of 8 to 14 GPa.
- D. C. Rubie *et al.*, *J. Geophys. Res.* **95**, 15829 (1990).
- A. Lacam, M. Madon, J.-P. Poirier, *Nature* **288**, 155 (1980).
- J.-N. Boland and L. Liu, *Geophys. Res. Lett.* **10**, 87 (1983).
- A. R. Remsberg, J. N. Boland, T. Gasparik, R. C. Liebermann, *Phys. Chem. Miner.* **15**, 498 (1988); A. R. Remsberg and R. C. Liebermann, *ibid.* **18**, 161 (1991).
- Interface-controlled growth involves short-range diffusion across the interface between the reactant and product phases. In contrast, diffusion-controlled growth involves changes in composition (for example, changes in the Fe/Mg ratio) that occur through long-range diffusion. Transformation of $(\text{Mg}, \text{Fe})_2\text{SiO}_4$ olivine to the β or γ phases might occur by the latter mechanism under near-equilibrium conditions in a two-phase stability field.
- M. Madon, F. Guyot, J. Peyronneau, J.-P. Poirier, *Phys. Chem. Miner.* **16**, 320 (1989).
- J. P. Poirier, *Geodynamics Series Vol. 4* (American Geophysical Union, Washington, DC, 1981), p. 113.
- The samples were contained in Mo capsules with a diameter and length of 1.5 mm. The pressure assembly was an MgO octahedron with a 10-mm edge length containing a cylindrical LaCrO_3 heater. Temperature was measured with a W3%Re-W25%Re thermocouple. The pressure was calibrated as a function of hydraulic oil pressure [D. Canil, *Phys. Earth Planet. Inter.* **86**, 25 (1994)]. The pressure uncertainty was ± 0.5 GPa.
- This design is in contrast to that of most earlier studies, in which relatively fine-grained polycrystalline starting materials were used. Enstatite was included in our samples to buffer the activity of SiO_2 during the reaction.
- T. Katsura and E. Ito, *J. Geophys. Res.* **94**, 15663 (1989).
- Hot-pressed starting materials were used because high densities of defects and submicrometer-sized grains that develop in pressurized powders are extremely reactive and therefore inappropriate for kinetic studies [A. J. Brearley, D. C. Rubie, E. Ito, *Phys. Chem. Miner.* **18**, 343 (1992)].
- The reason why the β phase is present in all reacted samples even though the experimental conditions nominally lie in the γ -phase stability field is not clear. Possible explanations are (i) that the estimated positions of the phase boundaries (Fig. 1) (22) might be in error; (ii) that the pressure calibration of the multianvil press may be in error because of the inclusion of the hot-pressing stage in our experiments; (iii) that the negative volume changes involved when olivine transforms to the high-pressure phases may reduce the pressure within the sample, at least on a localized scale, as the transformation proceeds; and (iv) that either the β phase or the γ phase could be metastable (25).
- D. C. Rubie and A. J. Brearley, *Nature* **348**, 628 (1990); A. J. Brearley and D. C. Rubie, *Phys. Earth Planet. Inter.* **86**, 45 (1994).
- M. Liu and R. A. Yund, *Phys. Earth Planet. Inter.* **89**, 177 (1995).
- D. L. Kohlstedt, C. Goetze, W. B. Durham, *The Physics and Chemistry of Minerals and Rocks*, R. G. J. Strens, Ed. (Wiley, New York, 1976), p. 35.
- M. Akaogi, E. Ito, A. Navrotsky, *J. Geophys. Res.* **94**, 15671 (1989).
- We thank C. Dupas for assistance with diffraction contrast imaging of stacking faults and dislocations, F. Seifert and S. Karato for helpful discussions, and H. Schulze for sample preparation. Supported by the Deutscher Akademischer Austauschdienst (A/95/09994) and the European Union "Human Capital and Mobility—Access to Large Scale Facilities" program (contract ERBCHGECT940053).

17 May 1996; accepted 9 August 1996